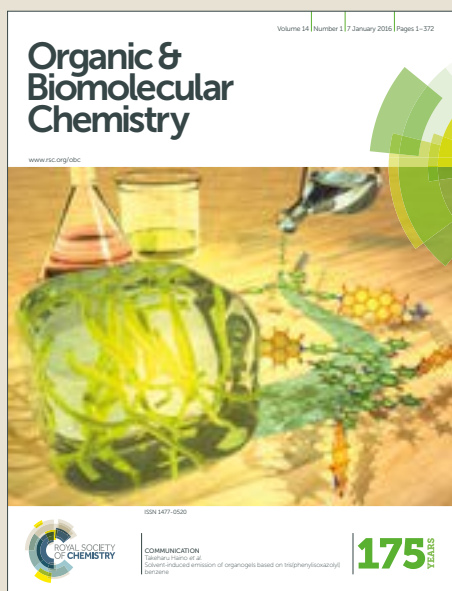


Organic & Biomolecular Chemistry

Accepted Manuscript



This article can be cited before page numbers have been issued, to do this please use: A. Y. Sukhorukov, V. Dorokhov, I. Golovanov, S. Ioffe and V. Tartakovskiy, *Org. Biomol. Chem.*, 2018, DOI: 10.1039/C8OB01039K.



This is an Accepted Manuscript, which has been through the Royal Society of Chemistry peer review process and has been accepted for publication.

Accepted Manuscripts are published online shortly after acceptance, before technical editing, formatting and proof reading. Using this free service, authors can make their results available to the community, in citable form, before we publish the edited article. We will replace this Accepted Manuscript with the edited and formatted Advance Article as soon as it is available.

You can find more information about Accepted Manuscripts in the [author guidelines](#).

Please note that technical editing may introduce minor changes to the text and/or graphics, which may alter content. The journal's standard [Terms & Conditions](#) and the ethical guidelines, outlined in our [author and reviewer resource centre](#), still apply. In no event shall the Royal Society of Chemistry be held responsible for any errors or omissions in this Accepted Manuscript or any consequences arising from the use of any information it contains.



Diastereoselective Synthesis and Profiling of Bicyclic Imidazolidinone Derivatives Bearing a Difluoromethylated Catechol Unit as Potent Phosphodiesterase 4 Inhibitors

Received 00th January 20xx,
Accepted 00th January 20xx

DOI: 10.1039/x0xx00000x

www.rsc.org/

Valentin S. Dorokhov,^{a,b} Ivan S. Golovanov,^a Vladimir A. Tartakovsky,^a Alexey Yu. Sukhorukov*^a and Sema L. Ioffe^a

Metal-mediated C-H functionalization of cyclic *N*-oxides was exploited to access a series of new difluoromethylated analogs of imidazolidinone-based PDE4 inhibitor **CMPI** in a diastereoselective manner. Among the products synthesized, compounds with fine-tuned activity/selectivity profiles as compared to both **CMPI** and the clinically applied Apremilast were identified. From these studies, an unusual fused 1,2-oxazinoimidazolidinone heterocyclic system was suggested as a novel scaffold for the design of potent and selective PDE4 inhibitors. Computational studies suggest that the oxygen atom in the imidazolidinone unit can bind to the metal ion center (most likely Mg²⁺). DFT calculations of the relative interaction energies of inhibitors with Mg²⁺ and Zn²⁺ ions were performed on a model of the bimetal active site of PDE4.

Introduction

Inhibitors of cAMP-specific type 4 phosphodiesterase (PDE4) have gained a considerable interest as potential drugs against inflammatory diseases, such as COPD, asthma, psoriatic arthritis, and some others.¹ PDE4 enzyme catalyses the hydrolysis of cyclic adenosine 3',5'-monophosphate (cAMP) in immune cells (neutrophils, macrophages, monocytes and T-cells), thereby regulating the concentration of this important second messenger. The decrease of intercellular cAMP levels as a result of PDE4 activity leads to the release of several pro-inflammatory mediators such as TNF- α , IL-12, IL-2 and LTB4. Inhibition of cAMP-specific PDE4 activity prevents the pro-inflammatory cell activation, and also reduces the dysfunction of structural lung cells, such as relaxation of airway smooth muscle.² Recently, PDE4 inhibitors Roflumilast (for treatment of COPD) and Apremilast (for treatment of psoriatic arthritis) were approved by FDA.^{1a,b}

However, most of PDE4 inhibitors, including those applied in clinic have dose-limiting gastric adverse effects, such as nausea, diarrhea and weight loss.³ These side effects are usually associated with non-selective inhibition of PDE4 isotypes, in particular PDE4D, which dominates over other

PDE4's in vomiting center of brain.^{1a,3c,4} Some potent PDE4 inhibitors, for example Cilomilast, are even more selective toward PDE4D as compared to other isotypes.^{1c} Thus, nowadays, a lot of research is being done toward the design of more potent and isotype-selective PDE4 inhibitors, preferably administered using the inhalation route.⁵ Notably, PDE4B isotype is considered to be an optimal target for the development of PDE4 inhibitors with high therapeutic index.

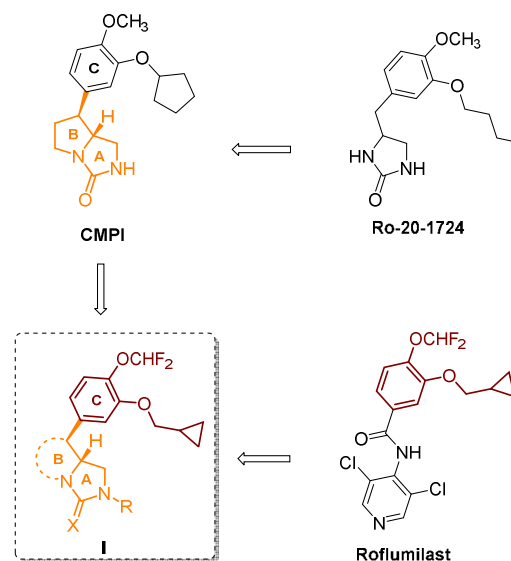


Figure 1. Difluoromethylated analogs of PDE4 inhibitor **CMPI**

Recently, we reported the first asymmetric synthesis and evaluation of both enantiomers of a highly potent PDE4

^a N. D. Zelinsky Institute of Organic Chemistry, 119991, Leninsky prospect, 47, Moscow, Russian Federation. E-mail: sukhorukov@ioc.ac.ru; Fax: +7 499 1355328; Tel: +7 499 1355329

^b Higher Chemical College of the Russian Academy of Sciences, D. Mendeleev University of Chemical Technology of Russia, 125047, Miusskaya sq., 9, Moscow, Russian Federation

Electronic Supplementary Information (ESI) available: Experimental procedures, copies of FTIR, NMR ¹H, ¹³C, ¹⁹F, COSY, HSQC, NOESY spectra of new compounds, details of biological assays, molecular docking and DFT calculations. See DOI: 10.1039/x0xx00000x

inhibitor **CMPI** (Figure 1),⁶ which was originally designed by GlaxoSmithKline as a strained analog of Ro-20-1724.⁷ Here, we used our synthetic strategy, improved by the recently developed transition metal-promoted methods for C-H functionalization of *N*-oxides,⁸ to access new difluoromethylated derivatives **I**, which combine the bicyclic imidazolidinone scaffold from **CMPI** (cycles **A**, **B**) and the aryl moiety of Roflumilast (catechol unit **C** in Figure 1). *In vitro/in vivo* evaluation of these compounds identified new potent PDE4 inhibitors with fine-tuned activity/selectivity profiles. These studies revealed structure-activity relationships throughout these series and provided insights into the binding pattern of cyclic urea fragment to the catalytic site of PDE4 enzymes.

Results and discussion

Structure design

The binding mode of catechol-based inhibitors is well defined with numerous co-crystal structures available for the complexes of PDE4B.⁹ The active site of PDE4B is comprised of three subunits, namely Q pocket (containing the glutamine switch and hydrophobic P-clamp), M pocket (containing a bimetal ion center) and S pocket (solvent-filled pocket). As can be seen from the crystal structure of PDE4B with Roflumilast (1XMU),⁹ the aryl unit is located in the Q pocket, making π - π stacking and hydrophobic interactions with P-clamp consisting of PHE446, ILE410, and PHE414 residues (Figure 2, (A)). Oxygen atoms of catechol unit are involved in a bidentate hydrogen bond with the γ -amide group of the GLU443 residue. Difluoromethyl group is located in Q₁ pocket formed by TYR233, ASN395, THR407, and TYR403, while the hydrophobic cyclopropylmethyl group lies across the Q₂ pocket (formed by residues MET411, MET431, and PHE414). Overall, the less electron-rich difluoromethoxy-substituted catechol in Roflumilast fits the lipophilic Q pocket better than the methoxy-substituted aryl in **CMPI**, Cilomilast and related PDE4 inhibitors.⁹ Moreover, an important advantage of OCHF₂ group over the methoxy-group is its ability to serve as a hydrogen bond donor^{10a} to the oxygen atom of THR407 residue as well as a counterpart in the multipolar interaction^{10b,c} with ASN395 residue (Figure 2, (B)).

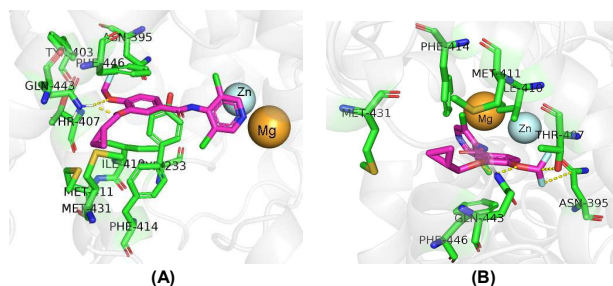


Figure 2. Binding modes of Roflumilast (crystal structure 1XMU). (A) Residues in Q pocket of PDE4B interacting with Roflumilast. (B) Close view on the difluoromethyl group making hydrogen bond with THR407 and multipolar interaction with ASN395. Large-size images can be found in Supporting information.

CMPI has a larger heterocyclic core (as compared to Roflumilast and Cilomilast), which can extend to the bimetal ion site (Figure 3, (A)). The bicyclic imidazolidinone unit with certain stereochemistry can exploit hydrophilic interactions with residues in M pocket (hydrogen bonds with ASP392 and HIS234), as well as direct metal-ligand coordination as can be judged from our previous docking studies.^{6a}

Substitution of aryl unit **C** in **CMPI** for the difluoromethylated catechol from Roflumilast was expected to increase the potency of the inhibitor. This was supported by docking of hybrid compound **1a** into the catalytic site of PDE4B using the crystal structure 1XMU (AutoDock Vina software was used,¹¹ see Supporting information for details and protocol). Compound **1a** showed more interactions as compared to **CMPI** and ca. 1 kcal/mol higher calculated affinity (Figure 3, (B)).

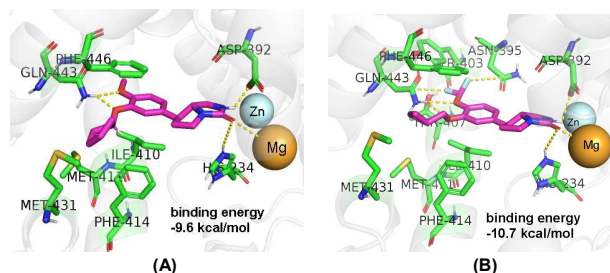


Figure 3. Molecular docking of **CMPI** and compound **1a** into the catalytic site of PDE4B (AutoDock Vina software). (A) Residues in Q and M pockets of PDE4B interacting with **CMPI** and the resulting affinity. (B) Residues in Q and M pockets of PDE4B interacting with **1a** and the resulting affinity. Large-size images can be found in Supporting information.

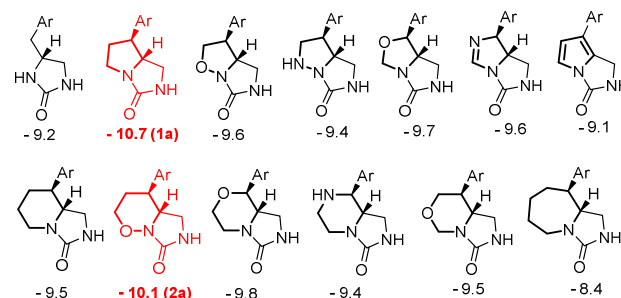


Figure 4. Calculated (docking) binding energies of various bicyclic imidazolidinones **I** in kcal/mol (AutoDock Vina software). Ar = 3-(cyclopropylmethoxy)-4-(difluoromethoxy)phenyl.

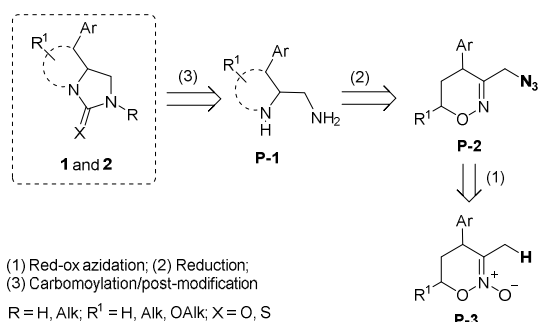
Since the size and type of heterocyclic ring **B** should influence binding in M pocket, we performed docking of predesigned structures **I** possessing various bicyclic imidazolidinone cores (selected examples are shown in Figure 4, see Supporting information for the full study). As can be seen from these studies, the increase of the size of ring **B**, as well as the introduction of heteroatoms and unsaturation resulted in the lowering of the predicted binding energy. However, apart from a pyrrolidine (**1a**), an unusual 1,2-oxazine ring (**2a**) was identified as a promising scaffold from this modeling. It should be noted, that no examples of 1,2-oxazine-based PDE4 inhibitors has been reported in the literature so far. On the

other hand, our recent studies revealed high potential of this scaffold for the design of anti-inflammatory compounds.¹²

Thus, pyrroloimidazolidinone **1a** and 1,2-oxazinoimidazolidinone **2a** were selected as target structures (Figure 4). In order to gain insights into effects of substituents in rings **A**, **B** and **C**, derivatives of **1a** and **2a** lacking the difluoromethyl group in catechol unit **C**, lacking NH hydrogen in ring **A** ($R \neq H$), having sulfur instead of carbonyl oxygen in ring **A** ($X = S$) and alkyl groups ($R^1 = \text{Alk}$) in the ring **B** were also synthesized (*vide infra*).

Synthetic strategy

The general strategy used to access target molecules **1** and **2** is shown in Scheme 1. According to this approach, the precursors of **1** and **2** are aminomethyl-substituted heterocycles **P-1**, which can be obtained by reduction of azido derivatives **P-2**. Controlled reduction of intermediates **P-2** would allow either to selectively reduce C=N bond with retaining of 1,2-oxazine ring, or to perform reductive contraction of the 1,2-oxazine to pyrrolidine cycle.¹³ Therefore, azides **P-2** can serve as precursors to both pyrroloimidazolidinone **1** and 1,2-oxazinoimidazolidinone **2** series of products.

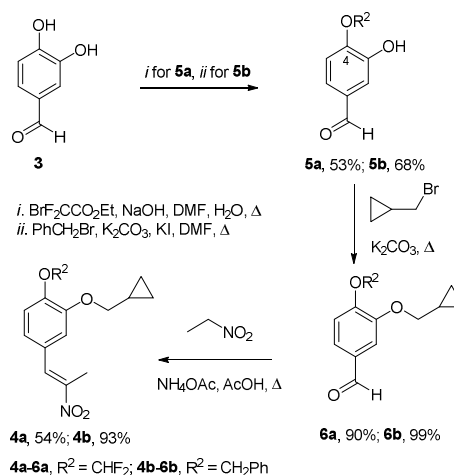


Scheme 1. Suggested synthetic strategy to compounds **1** and **2**

Similar strategy was used in the synthesis of **CMPI** enantiomers,^{6a} yet here we attempted to use the advantage of our recently developed transition metal promoted red-ox C–H activation of cyclic *N*-oxides of type **P-3**.⁸ Moreover, it was not evident, whether this methodology is tolerated by electron-deficient difluoromethyl group.

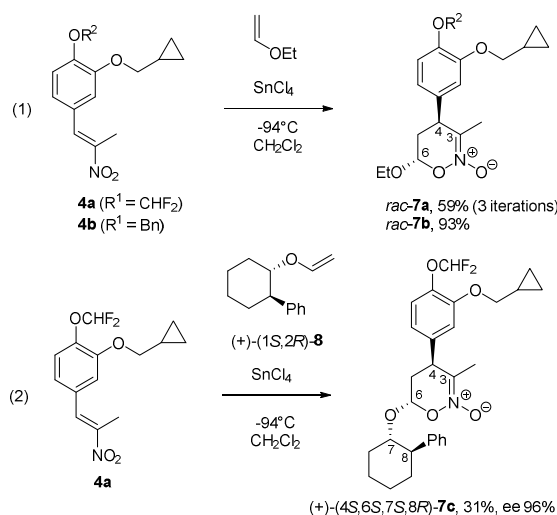
Diastereoselective synthesis of pyrroloimidazolidinone series

Initially, the synthesis of hitherto unknown nitroalkenes **4a** and **4b** was performed from protocatechuic aldehyde **3** according to the general route shown in Scheme 2. At the first stage, the more acidic hydroxyl group at the C-4 position in **3** was difluoromethylated or benzylated using standard protocols,¹⁴ which gave aldehydes **5a** and **5b**, respectively. Subsequent alkylation of the free OH group in **5** with bromomethylcyclopropane in the presence of K_2CO_3 furnished aldehydes **6**. Condensation of the latter with nitroethane catalyzed by ammonium acetate afforded nitroalkenes **4a** and **4b**.



Scheme 2. Synthesis of nitroalkenes **4a** and **4b** from protocatechuic aldehyde

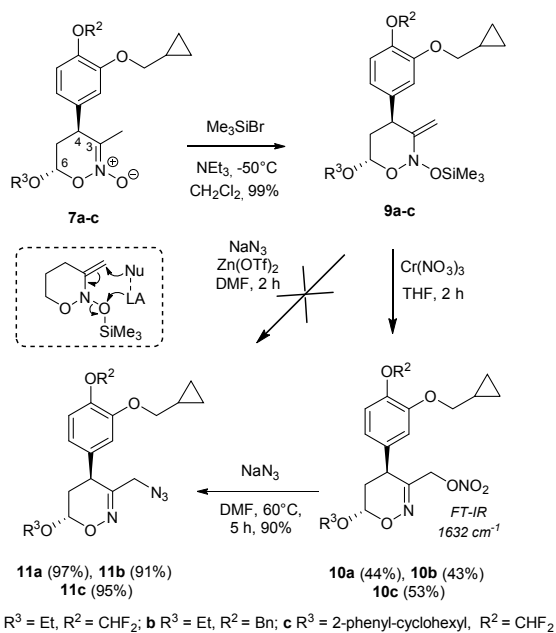
On the next stage, racemic 1,2-oxazine-*N*-oxides **7a** and **7b** were assembled by the inverse electron demand [4+2]-cycloaddition of nitroalkenes **4a** or **4b** with ethyl vinyl ether promoted by tin tetrachloride (eq. (1), Scheme 3). Remarkably, in contrast to nitrostyrene **4b**, the difluoromethylated derivative **4a** entered cycloaddition with poor conversion. This can be attributed to its lesser ability to form a reactive complex with $SnCl_4$ because of a more electron-deficient character of aryl group.¹⁵ The unreacted nitroalkene **4a** could be recovered and subsequently used in the cycloaddition. After three repeated iterations, the desired nitronate **7a** was obtained in acceptable 59% yield based on the nitroalkene **4a**.



Scheme 3. Synthesis of 1,2-oxazine-*N*-oxides **7a-c**

The enantiomerically pure cyclic nitronate **7c**, a precursor of (7*S*,7*aR*)-enantiomer of **1a**, was prepared employing *trans*-1-phenyl-2-(vinylloxy)cyclohexane (1*S*,2*R*-**8**) as chiral auxiliary (eq. (2), Scheme 3).⁶ Only two of four possible stereoisomers of nitronate **7c** were formed with one being predominant (*dr* = 9 : 1). The major isomer was isolated by column

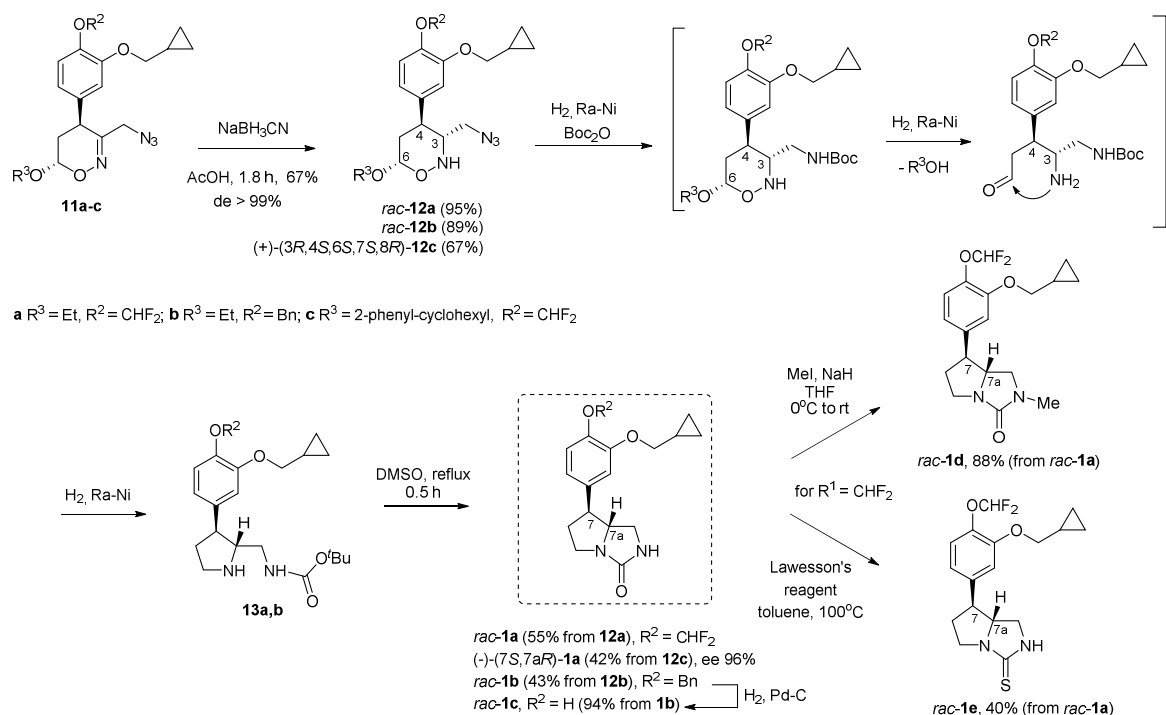
chromatography with high diastereomeric and enantiomeric purity (de 94%, ee 96%).¹⁶



Scheme 4. Synthesis of azides **11a-c**

Having prepared both racemic and enantiomerically enriched nitronates **7**, we then proceeded with azidation of the methyl group at the C-3 atom (Scheme 4). Recently, we reported a

novel approach to achieve selective functionalization of α -position in nitronates based on their transformation into *N*-silyloxyenamines and subsequent reaction with nucleophiles in the presence transition metal Lewis acids.⁸ Following this method, *N*-silyloxyenamines **9a-c** were prepared in almost quantitative yields by silylation of nitronates **7a-c** (Scheme 4). However, interaction of enamines **9** with $\text{NaN}_3/\text{Zn}(\text{OTf})_2$ system^{8c} produced only complex mixtures of products.¹⁷ Fortunately, we were able to introduce the nitroxy-group using the recently developed Cr(III)-promoted addition of the nitrate anion to *N*-silyloxyenamines of type **9**.^{8a,18} Subsequent nucleophilic substitution of the nitroxy-group for the azide anion provided azides **11a-c** in high yields (Scheme 4). On the next stage, the stereocenter at the C-3 atom in azides **11** was installed by $\text{NaBH}_3\text{CN}/\text{AcOH}$ reduction, which produced exclusively 3,4-*trans*-isomers of corresponding tetrahydro-1,2-oxazines **12a-c** (Scheme 5). Hydrogenation of these 1,2-oxazines over Raney nickel catalyst in the presence of Boc_2O gave aminomethyl-substituted pyrrolidines **13a** and **13b** via a domino-process involving successive reduction/protection of azido-group, cleavage of the N–O bond, and intramolecular reductive amination to give a pyrrolidine ring (Scheme 5). Interestingly, benzyloxy group in **12b** was not cleaved under these conditions. The resulting Boc-protected pyrrolidines **13** (without purification) were cyclized into target pyrroloimidazolidinones *rac*-**1a** and **1b** upon gentle reflux in DMSO. Enantiomerically pure product (–)-(7*S*,7*aR*)-**1a** (96% ee) was obtained in a same manner from azide **12c** (Scheme 5).



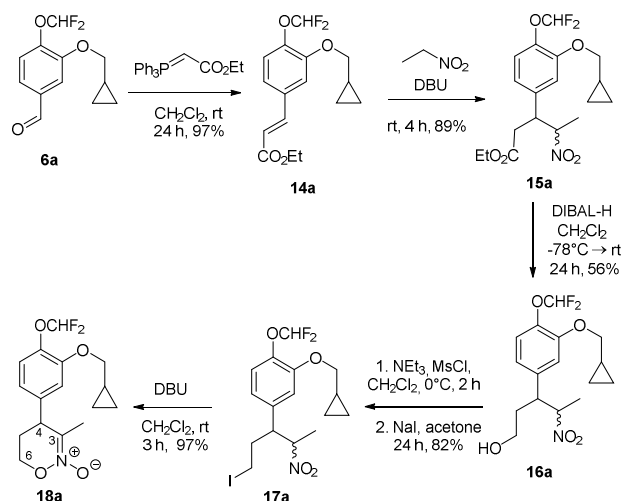
Scheme 5. Synthesis of target compounds **1a-e** from azides **11a-c**

The synthesis of free phenol **1c** was accomplished by catalytic reductive debenzoylation of pyrroloimidazolidinone *rac*-**1b** over Pd-C (Scheme 5). Unfortunately, we were not able to perform difluoromethylation of phenol **1c** to give product **1a** using BrF₂CCO₂Et/NaOH as well as the recently developed TMSCF₂Br/KOH system,¹⁹ likely because of a competitive addition of difluorocarbene to the N–H unit.

Racemic pyrroloimidazolidinone **1a** was further modified by methylation of carbamide nitrogen to give product **1d** and by transformation of carbamide into thiocarbamide with Lawesson's reagent (product **1e**) (Scheme 5).

Diastereoselective synthesis of 1,2-oxazinoimidazolidinone series

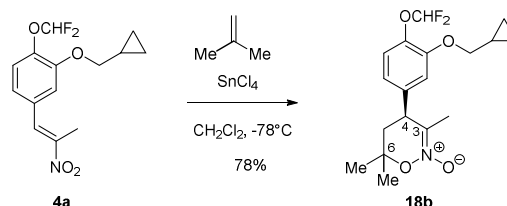
Fused 1,2-oxazinoimidazolidine heterocyclic system was not known in the literature, and no strategies for its assembly have been developed so far. To synthesize the proposed 1,2-oxazine-based structure **2a** possessing an extra oxygen atom in the ring **B**, 1,2-oxazine-*N*-oxide **18a** unsubstituted at C-6 position is needed (Scheme 6). The synthesis of this intermediate cannot be achieved by a conventional [4+2]-cycloaddition used to prepare 1,2-oxazine-*N*-oxides **7** (Scheme 3), since ethylene does not react with nitroalkenes.



Scheme 6. Synthesis of nitronate **18a**

Accordingly, nitronate **18a** was prepared in a step-wise manner through the cyclization of δ -iodo-substituted nitro compound **17a**. The synthesis of the latter was accomplished starting from aldehyde **6a**, which was transformed into unsaturated ester **14a** on the first stage by Wittig olefination. Michael addition of nitroethane to **14a** in the presence of DBU furnished the corresponding nitroester **15a** as an equimolar mixture of diastereomers. Nitroesters **15a** were transformed into iodides **17a** by the DIBAL-H reduction of ester and subsequent mesylation of alcohols **16a** followed by treatment with NaI in acetone. Smooth cyclization of isomeric iodides **17a** to nitronate **18a** was achieved upon the action of DBU in CH₂Cl₂ in nearly quantitative yield.

Nitronate **18b**, which is the intermediate in the synthesis of 2,2-dimethyl-substituted derivative of **2a**, was prepared in a straightforward way by the SnCl₄-promoted [4+2]-cycloaddition of nitroalkene **4a** to 2-methylpropene (Scheme 7). Interestingly, unlike the reaction with ethyl vinyl ether, no significant effect of difluoromethyl group on the reactivity and conversion was found in this case (cf. Scheme 3, eq. (1) and Scheme 7). This is likely because cationic polymerization of 2-methylpropene is much slower as compared to vinyl ethers.

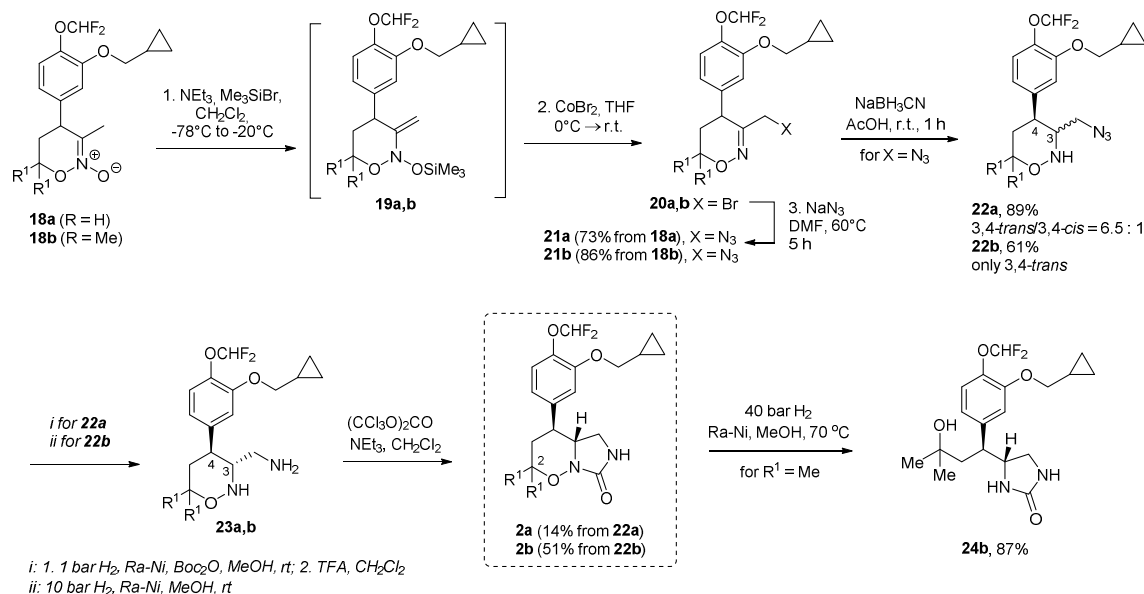


Scheme 7. Synthesis of nitronate **18b**

Functionalization of the methyl group at the C-3 position in *N*-oxides **18** was accomplished in a similar manner to nitronates **7** (Scheme 8), yet the initial introduction of bromide proved to be more advantageous as compared to the nitrate anion in this case. Thus, silylation of *N*-oxides **18a** and **18b** with TMSBr/Et₃N followed by treatment of intermediate *N*-silyloxyamines **19a** and **19b** with CoBr₂ in THF furnished bromides **20a** and **20b**.^{8b} The latter were reacted with NaN₃ in DMF without purification to give azidomethyl-substituted 1,2-oxazines **21a,b** in 73–86% yields from nitronates **18**. Reduction of **21a** with NaBH₃CN in acetic acid provided tetrahydro-1,2-oxazine **22a** as a mixture of diastereomers in 6.5 : 1 ratio in favor of desired 3,4-*trans*-isomer. Analogous reduction product **21b** gave single isomer of the corresponding reduction product **22b** (Scheme 8).

Final stage of the synthesis was the construction of imidazolidinone ring **A**. The major challenge here was to reduce azido-group leaving the N–O bond intact (Scheme 8). Catalytic hydrogenation of **22a** even under very mild conditions (1 bar H₂, Ra-Ni) led to the reduction of both groups. Fortunately, we found, that protection of the NH₂-group (arising from azide) with Boc resulted in somewhat decrease of the rate of N–O bond hydrogenolysis. Thus, mild hydrogenation of oxazine **22a** over Raney nickel in the presence of Boc₂O afforded Boc-protected derivative of amine **23a**. The latter was transformed into target bicyclic derivative **2a** by deprotection with TFA followed by treatment with triphosgene/Et₃N system.

Reduction of the azido-group in the more sterically hindered intermediate **22b** was less problematic. Almost no cleavage of 1,2-oxazine ring was observed even when hydrogenation was performed at elevated hydrogen pressure. Interaction of the resulting amine **23b** with triphosgene/Et₃N afforded the desired product **2b** in good overall yield of 51% from **22b**. Hydrogenolysis of N–O bond in 1,2-oxazine **2b** at elevated temperature and pressure afforded the open-chain derivative **24b** in high yield (Scheme 8).

Scheme 8. Synthesis of target compounds **2a,b** and **24b** from cyclic nitronates **18a** and **18b****In vitro** PDE4B1 inhibition studies

All synthesized compounds were tested for their ability to inhibit FAM-cAMP hydrolysis catalyzed by recombinant human PDE4B1 using a standard *in vitro* enzymatic assay.²⁰ Clinically applied PDE4 inhibitor Apremilast^{1a,b} was used as a reference compound in these studies. The results are summarized in Table 1.

Table 1. IC_{50} values for synthesized products and reference compounds (PDE4B1)

Compound	IC_{50} , nM
<i>rac</i> - 1a	18
(7 <i>S</i> ,7 <i>aR</i>)- 1a	17
<i>rac</i> - 1b	> 10000
<i>rac</i> - 1c	3200
<i>rac</i> - 1d	25
<i>rac</i> - 1e	59
<i>rac</i> - 2a	39
<i>rac</i> - 2b	1000
<i>rac</i> - 24b	> 10000
Apremilast (reference compound)	18
CMPI	27 ^{6a}
Roflumilast	ca. 1 ²¹
Ro-20-1724	ca. 2000 ⁷

As can be seen from the data in Table 1, racemic compound *rac*-**1a** exhibits higher potency than *rac*-CMPI, and comparable to the activity of clinically used PDE4 inhibitor Apremilast (yet lower than Roflumilast). Single enantiomer (7*S*,7*aR*)-**1a** has essentially the same activity as the racemate suggesting that the eudysmic ratio is ca. 1 (unlike CMPI, which enantiomers differ considerably in the inhibitory activity^{6a}).

The presence of difluoromethoxy group in ring C is essential for high inhibitory activity as can be seen from the IC_{50} values of products **1b** and **1c** bearing OBn and OH groups instead of

OCHF₂ fragment. Almost no activity in case of **1b** can be attributed to the sterical hindrance of benzyl-substituted catechol unit, which does not fit the lipophilic Q pocket of the enzyme.

Analysis of 1,2-oxazinoimidazolone series **2** allows to shed some light on the effect of the ring B and the substitution in it on the PDE4B inhibition activity. Thus, the replacement of the pyrrolidine ring in **1a** by 1,2-oxazine cycle results in about twofold decrease in IC_{50} value. Addition of two methyl groups to the 1,2-oxazine ring (position C-2, product **2b**) leads to a dramatic drop of the activity to IC_{50} 1 μM . Opening of 1,2-oxazine ring results in almost complete disappearance of the inhibition activity (IC_{50} > 10 μM for product **24b**). This demonstrates that the presence of ring B may be important for retaining high potency (cf. with low potent Ro-20-1724, Table 1, Figure 1).

Surprisingly, introduction of methyl group at the nitrogen atom of the imidazolidinone ring in **1a** resulted in a slight decrease of activity only (cf. **1a** and **1d** in Table 1). Substitution of carboxamide oxygen atom for sulfur led to a more noticeable drop of inhibitory activity (cf. **1a** and **1e** in Table 1). These results suggest that the N-H hydrogen bond donor in the imidazolidinone ring is not essential for binding of inhibitor. From the docking of **1a** it can be assumed that C=O group binds to the metal ion, most likely Mg^{2+} (Figure 5, (A)). In the top scoring docking pose of **1a**, carbonyl group points directly onto the magnesium ion with the relatively close calculated Mg-O distance of 3.0 Å.

Metalloprotein-ligand interactions are rarely observed for PDE4 inhibitors in crystal structures. A characteristic example is the complex of PDE4D with Zardaverine (1XOR, Figure 5, (B)), in which ligand's carbonyl group occupies one coordination site of Zn^{2+} instead of a water molecule.⁹ Metal-

ligand binding may play an important role in the inhibition of PDE4 since it would block the access of cAMP to the catalytic domain of the enzyme. We were interested in the energy of this interaction, since it is not adequately estimated by docking software with nonpolarized molecular force field methods. Therefore, we performed DFT-calculations of binding of Zardaverine and ligands **1a'**, **1e'** (compounds **1a** and **1e** without the aryl group) to magnesium and zinc ions using a model of the catalytic site of PDE4 (Table 2).

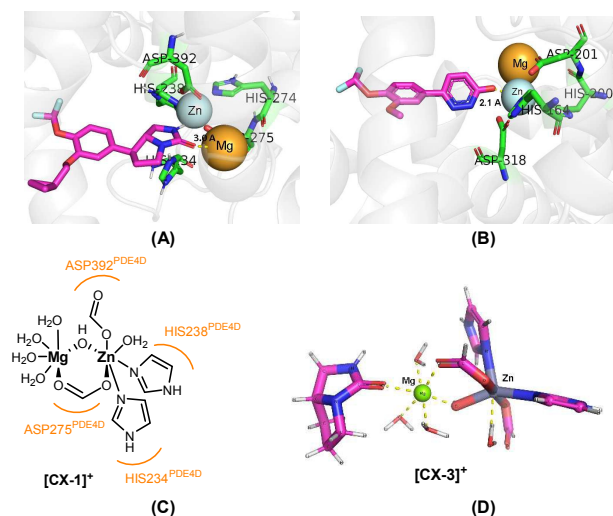


Figure 5. Metalloprotein-ligand interactions for PDE4 inhibitors. (A) Docking of **1a** into the catalytic site of PDE4B (close view on the interactions in M pocket). (B) Interaction of Zardaverine with the Zn²⁺ ion in M pocket of PDE4D (crystal structure 1XOR). (C) DFT model of PDE4 bimetallic catalytic site. (D) Computed geometry of complex of **1a'** with the model of PDE4 bimetallic catalytic site (MN15L/Def2TZVP, smd, H₂O). Large-size images can be found in Supporting information.

Table 2. Calculated binding energies of ligands to the metal ion in CX-1

$$[\text{CX-1}]^+ + \text{L} \rightleftharpoons [\text{CX-n}]^+ + \text{H}_2\text{O}$$

Ligand	Calculated ΔG° of binding to metal, kcal/mol ^a	
	Mg ²⁺ (opt complex ^b)	Zn ²⁺ (opt complex ^b)
Zardaverine	-	-7.9 [CX-2] ⁺
1a'	-3.8 [CX-3] ⁺	-3.4 [CX-4] ⁺
1e'	+1.7 [CX-5] ⁺	-3.1 [CX-6] ⁺

^a Defined as calculated ΔG° of substitution of water molecule for ligand. ^b For DFT-optimized structures of complexes [CX-n]⁺ see Supporting information. All complexes were characterized by only real vibrational frequencies.

The development of a theoretic model of the bimetallic catalytic site was performed at MN15L/Def2TZVP (smd, H₂O) level of theory using crystallographic structure 1XOR (Figure 5, (B)) as an initial approximation. In our model, histidines HIS164 and HIS200 were changed to imidazole rings, ASP201 and ASP318 residues were simplified to formate ions, the bridge oxygen atom was treated as hydroxyl group,²² water molecules were left on the metal ions (Figure 5, (C)). Geometry of the resulting complex [CX-1]⁺ was optimized and vibrational analysis was performed, which revealed no imaginary frequencies.

Binding energies were calculated as ΔG° of substitution of water molecule for ligand either on zinc or magnesium ions in the optimized complex [CX-1]⁺ (Table 2).²³ As can be seen from this data, oxygen binding ligand **1a'** almost equally favorable interacts with either magnesium or zinc centers, yet sulfur binding ligand **1e'** can efficiently interact only with Zn²⁺ (coordination of Mg²⁺ is unfavourable). Overall, the energy of metal-ligand interactions may significantly contribute to the binding of ligands to the active site of PDE4 enzyme (ΔG° -3 - -8 kcal/mol) and this should be taken into account in the design of new PDE4 inhibitors. Using our theoretic model, the energy of these interactions can be easily calculated by DFT methods.

PDE4 selectivity studies *in vitro*

PDE4 isoforms have highly conserved catalytic domain, yet contain multiple differentially spliced exons and unique N-terminal regions. Classical PDE4 inhibitors typically do not exhibit any selectivity across PDE4 isoforms. On the other hand, different intercellular location of these isoforms allows for modulation of cAMP signaling in specific cells by an isoform-selective inhibitor.

For the most active compounds **1a**, **1d**, **1e** and **2a** the selectivity of inhibition on a panel of 9 isotype PDE4 was examined in comparison with the reference drug Apremilast and PDE4 inhibitor **CMPI** (Figure 6). As can be seen from this data, apremilast does not exhibit any selectivity across the PDE4 isotype panel, whereas **CMPI** is twice less active towards PDE4C enzyme as compared to other isotypes. On the other hand, compounds **1a** and, especially, 1,2-oxazine **2a** show more interesting selectivity profiles. Both compounds are significantly less potent for inhibition of PDE4C (**2a** is ca. ten-times more active towards PDE4B1 compared to PDE4C1). Furthermore, somewhat higher activity is observed for PDE4B isotypes as compared to PDE4D isotypes. This is opposite to the selectivity profile of well-known PDE4 inhibitor Cilomilast, which is more PDE4D-selective.^{1c} Overall, as can be judged from the Gini coefficients G_{0,1},²⁴ compounds **1a** and **2a** show much better selectivity profiles than Apremilast and **CMPI**. It can be expected that one of enantiomers of 1,2-oxazine **2a** may have even higher activity and selectivity index.

Another interesting point is the higher activity of **1a** and, especially **2a**, towards the long isoform PDE4D7 (possessing a unique N-terminal region) compared to another long isoform PDE4D3 and short isoform PDE4D2. Although this requires special studies, we may speculate that some specific interactions of the ligand with the residues outside the catalytic site take place in a specific "capped" conformation of PDE4D7.²⁵

For N-methylated compound **1d** and cyclic thiourea derivative **1e** the selectivity picture is similar to **CMPI**. This suggests that the imidazolidinone ring with an N-H hydrogen bond donor may be important for distinguishing PDE4 isoforms.

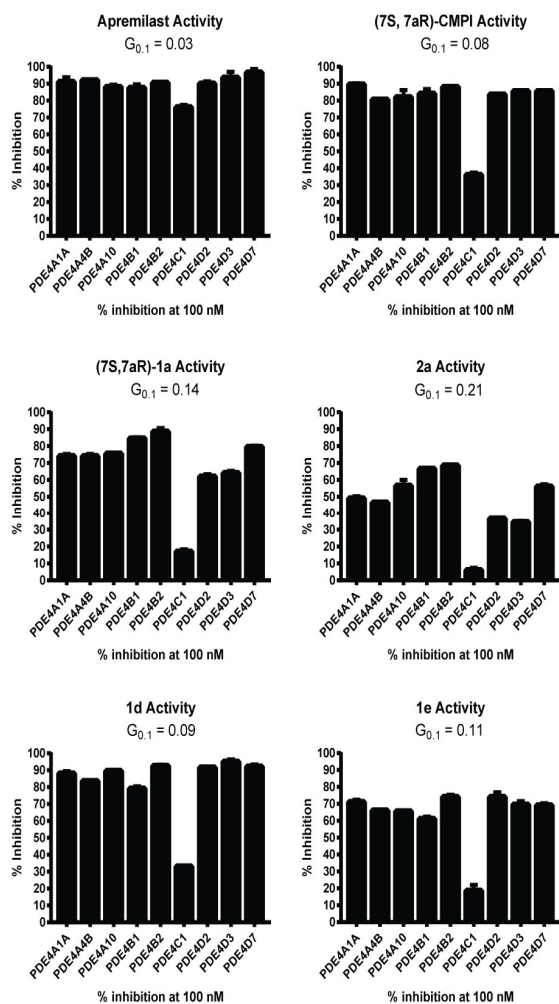


Figure 6. PDE4 inhibition selectivity diagrams. $G_{0.1}$ – Gini coefficient at $0.1 \mu\text{M}^{24}$

PDE4B inhibition studies *in vivo*

For two potent compounds **1a** and **2a**, a PDE4B cell signaling pathway assay was performed. *In vivo* PDE4B inhibition activity was measured using a cell-based CRE luciferase reporter assay in comparison with Apremilast. In these experiments cells were co-transfected with PDE4B and CRE luciferase reporter. Intracellular levels of cAMP were monitored *via* expression of luciferase from the CRE reporter, acting as an intracellular cAMP sensor.

Table 3. EC₅₀ values for compounds **1a** and **2a** obtained in a cellular assay

Compound	EC ₅₀ , μM
1a	1.4
2a	> 10
Apremilast	2.8

The results of these studies (Table 3) revealed that **1a** is twice more potent than Apremilast, yet the 1,2-oxazine-based compound **2a** exhibited poor activity in this experiment.

Conclusions

In conclusion, we developed a general route to difluoromethylated analogs of potent imidazolidinone-based PDE4 inhibitor **CMPI** employing efficient C-H functionalizations of 1,2-oxazine-*N*-oxides. A series of **CMPI** analogs possessing structural modifications in rings **A**, **B** and **C** were synthesized in diastereoselective manner. Structure-activity/selectivity relationships throughout these series were studied and compounds with fine-tuned activity/selectivity profiles compared to both **CMPI** and the clinically applied Apremilast were identified. From these studies, an unusual bicyclic 1,2-oxazine-based heterocyclic system was suggested as a novel scaffold for the design of selective and potent PDE4 inhibitors. Biological studies in combination with docking and DFT calculations provided important insights into the binding pattern of bicyclic urea unit to the M pocket of the catalytic site in PDE4 enzymes. DFT calculations of the energy of metal-ligand interaction on a model of PDE4 bimetallic active site were performed. Calculations suggest that metal-ligand interactions may play a pivotal role in binding to the active site of PDE4 enzyme.

Conflicts of interest

There are no conflicts to declare.

Acknowledgements

The financial support from Russian Foundation for Basic Research (grant 17-33-80172_mol_ev) is greatly acknowledged. Authors thank Dr. Yulia Khoroshutina and Dr. Roman Novikov for taking 2D NMR spectra, Mr. Kevin Kurtz and Mr. Kenneth D'Arigo from BPS Bioscience for conducting standard PDE4 inhibition assays on a contract basis.

Notes and references

- a) A. Gavalda and R. S. Roberts, *Expert Opin. Ther. Pat.* **2013**, *23*, 997-1016; b) M. Mazur, J. Karczewski, M. Lodyga, R. Zaba and Z. Adamski, *J. Dermatol. Treat.* **2015**, *26*, 326-328; c) J. M. Michalski, G. Golden, J. Ikari and S. I. Rennard, *Clin. Pharmacol. Ther.* **2012**, *91*, 134-142; d) A. M. Mulhall, C. A. Droegge, N. E. Ernst, R. J. Panos and M. A. Zafar, *Expert Opin. Investig. Drugs* **2015**, *24*, 1597-1611; e) C. P. Page and D. Spina, *Curr. Opin. Pharm.* **2012**, *12*, 275-286; f) G. Song, X. Zhu, J. Li, D. Hu, D. Zhao, Y. Liao, J. Lin, L.-H. Zhang and Z.-N. Cui, *Bioorg. Med. Chem.*, **2017**, *25*, 5709-5717; g) S. Guariento, A. Karawajczyk, J. A. Bull, G. Marchini, M. Bielska, X. Iwanowa, O. Bruno, P. Fossa and F. Giordanetto, *Bioorg. Med. Chem. Lett.*, **2017**, *27*, 24-29; h) J.-S. Zhang, X. Liu, J. Weng, Y.-Q. Guo, Q.-J. Li, A. Ahmed, G.-H. Tang and S. Yin, *Org. Chem. Front.*, **2017**, *4*, 170-177; i) B. S. Chinta and B. Baire, *Org. Biomol. Chem.*, **2017**, *15*, 5908-5911.
- a) M. D. Houslay, G. S. Baillie and D. H. Maurice, *Circul. Res.* **2007**, *100*, 950-966; b) A. Kodimuthali, S. S. L. Jabaris and M. Pal, *J. Med. Chem.* **2008**, *51*, 5471-5489.
- a) B. Beghè, K. F. Rabe and L. M. Fabbri, *Am. J. Respir. Crit. Care Med.* **2013**, *188*, 271-278; b) W. M. Brown, *Int. J. Chron. Obstruct. Pulmon. Dis.* **2007**, *2*, 517-533; c) A. Robichaud, P.

- B. Stamatiou, S. L. C. Jin, N. Lachance, D. MacDonald, F. Laliberté, S. Liu, Z. Huang, M. Conti and C.-C. Chan, *J. Clin. Invest.* **2002**, *110*, 1045-1052.
- 4 a) J. A. Cherry and R. L. Davis, *J. Comp. Neurol.* **1999**, *407*, 287-301; b) X. Miró, S. Pérez-Torres, P. Puigdomènech, J. M. Palacios and G. Mengod, *Synapse* **2002**, *45*, 259-269; c) F. Mori, S. Pérez-Torres, R. De Caro, A. Porzionato, V. Macchi, J. Beleta, A. Gavalda, J. M. Palacios and G. Mengod, *J. Chem. Neuroanat.* **2010**, *40*, 36-42.
- 5 a) L. Carzaniga, G. Amari, A. Rizzi, C. Capaldi, R. De Fanti, E. Ghidini, G. Villetti, C. Carnini, N. Moretto, F. Facchinetti, P. Caruso, G. Marchini, L. Battipaglia, R. Patacchini, V. Cenacchi, R. Volta, F. Amadei, A. Pappani, S. Capacchi, V. Bagnacani, M. Delcanale, P. Puccini, S. Catinella, M. Civelli and E. Armani, *J. Med. Chem.* **2017**, *60*, 10026-10046; b) R. S. Roberts, S. Sevilla, M. Ferrer, J. Taltavull, B. Hernández, V. Segarra, J. Gràcia, M. D. Lehner, A. Gavalda, M. Andrés, J. Cabedo, D. Vilella, P. Eichhorn, E. Calama, C. Carcasona and M. Miralpeix, *J. Med. Chem.*, **2018**, *61*, 2472-2489.
- 6 a) P. A. Zhmurov, A. Y. Sukhorukov, V. I. Chupakhin, Y. V. Khomutova, S. L. Ioffe and V. A. Tartakovsky, *Org. Biomol. Chem.* **2013**, *11*, 8082-8091; b) A. Y. Sukhorukov, Y. D. Boyko, S. L. Ioffe, Y. A. Khomutova, Y. V. Nelyubina and V. A. Tartakovsky, *J. Org. Chem.*, **2011**, *76*, 7893-7900.
- 7 M. F. Brackeen, J. A. Stafford, D. J. Cowan, P. J. Brown, P. L. Domanico, P. L. Feldman, D. Rose, A. B. Strickland, J. M. Veal and M. Verghese, *J. Med. Chem.* **1995**, *38*, 4848-4854.
- 8 a) Y. A. Naumovich, V. E. Buckland, D. A. Sen'ko, Y. V. Nelyubina, Y. A. Khoroshutina, A. Y. Sukhorukov and S. L. Ioffe, *Org. Biomol. Chem.* **2016**, *14*, 3963-3974; b) A. Y. Sukhorukov, M. A. Kapatsyna, T. L. T. Yi, H. R. Park, Y. A. Naumovich, P. A. Zhmurov, Y. A. Khomutova, S. L. Ioffe and V. A. Tartakovsky, *Eur. J. Org. Chem.* **2014**, 8148-8159; c) P. A. Zhmurov, Y. A. Khoroshutina, R. A. Novikov, I. S. Golovanov, A. Y. Sukhorukov and S. L. Ioffe, *Chem. - Eur. J.* **2017**, *23*, 4570-4578.
- 9 G. L. Card, B. P. England, Y. Suzuki, D. Fong, B. Powell, B. Lee, C. Luu, M. Tabrizizad, S. Gillette, P. N. Ibrahim, D. R. Artis, G. Bollag, M. V. Milburn, S.-H. Kim, J. Schlessinger and K. Y. J. Zhang, *Structure* **2004**, *12*, 2233-2247.
- 10 (a) J. A. Erickson and J. I. McLoughlin, *J. Org. Chem.*, **1995**, *60*, 1626-1631; (b) P. Zhou, J. Zou, F. Tian and Z. Shang, *J. Chem. Inf. Model.*, **2009**, *49*, 2344-2355; (c) K. Müller, C. Faeh and F. Diederich, *Science*, **2007**, *317*, 1881-1886.
- 11 O. Trott and A. J. Olson, *J. Comput. Chem.*, **2010**, *31*, 455-461.
- 12 a) A. C. Nirvanappa, C. D. Mohan, S. Rangappa, H. Ananda, A. Y. Sukhorukov, M. K. Shanmugam, M. S. Sundaram, S. C. Nayaka, K. S. Girish, A. Chinnathambi, M. E. Zayed, S. A. Alharbi, G. Sethi, Basappa and K. S. Rangappa, *PLoS One* **2016**, *11*, e0163209; b) A. Y. Sukhorukov, A. C. Nirvanappa, J. Swamy, S. L. Ioffe, S. Nanjunda Swamy, Basappa and K. S. Rangappa, *Bioorg. Med. Chem. Lett.* **2014**, *24*, 3618-3621.
- 13 A. Y. Sukhorukov and S. L. Ioffe, *Chem. Rev.* **2011**, *111*, 5004-5041.
- 14 S. Zheng, G. Kaur, H. Wang, M. Li, M. Macnaughtan, X. Yang, S. Reid, J. Prestegard, B. Wang and H. Ke, *J. Med. Chem.*, **2008**, *51*, 7673-7688.
- 15 For the mechanism see: S. E. Denmark, B. S. Kesler and Y. C. Moon, *J. Org. Chem.*, **1992**, *57*, 4912-4924.
- 16 The (4*S*,6*S*,7*S*,8*R*)-configuration of major isomer **7c** was reasonably proposed based on our previous studies on [4+2]-cycloadditions with vinyl ether **8**.^{6b}
- 17 In the ¹H NMR spectra, the characteristic H-6 proton was absent indicating that the acetal unit at C-6 is cleaved.
- 18 Slight epimerization of C-6 center was observed in the case of enantiopure nitrate **10c** (d.r. 4.5 : 1), yet the epimer could be separated on the next stages.
- 19 L. Li, F. Wang, C. Ni and J. Hu, *Angew. Chem. Int. Ed.* **2013**, *52*, 12390-12394.
- 20 P. H. Schafer, A. Parton, L. Capone, D. Cedzik, H. Brady, J. F. Evans, H. W. Man, G. W. Muller, D. I. Stirling and R. Chopra, *Cell. Signal.*, **2014**, *26*, 2016-2029.
- 21 A. Hatzelmann, E. J. Morcillo, G. Lungarella, S. Adnot, S. Sanjar, R. Beume, C. Schudt and H. Tenor, *Pulm. Pharmacol. Ther.*, **2010**, *23*, 235-256.
- 22 a) C.-G. Zhan and F. Zheng, *J. Am. Chem. Soc.* **2001**, *123*, 2835-2838; b) K. Y. Wong and J. Gao, *FEBS J.* **2011**, *278*, 2579-2595.
- 23 V. Sladek and I. Tvaroška, *J. Phys. Chem. B*, **2017**, *121*, 6148-6162.
- 24 P. P. Graczyk, *J. Med. Chem.*, **2007**, *50*, 5773-5779.
- 25 a) J. P. Day, B. Lindsay, T. Riddell, Z. Jiang, R. W. Allcock, A. Abraham, S. Sookup, F. Christian, J. Bogum, E. K. Martin, R. L. Rae, D. Anthony, G. M. Rosair, D. M. Houslay, E. Huston, G. S. Baillie, E. Klusmann, M. D. Houslay and D. R. Adams, *J. Med. Chem.* **2011**, *54*, 3331-3347; b) D. Fox, A. B. Burgin and M. E. Gurney, *Cell. Signal.* **2014**, *26*, 657-663.